A GENERALIZED DEPENDENCE OF DETONATION VELOCITY ON CHARGE DIAMETER INCLUDING LOW VELOCITY DETONATION

Ermolaev B. S. (1), Khasainov B. A. (2), and Presles H.-N. (2)

(1) Semenov Institute of Chemical Physics, RAS, Moscow, Russia
(2) Laboratoire de Combustion et de Détonique, UPR CNRS 9028, ENSMA, Poitiers, France

ABSTRACT

According to experimental data available for high explosives, dependence of detonation velocity on charge diameter *D(d)* comprises two separate branches for low velocity and normal detonations. In an intermediate velocity range steady detonations are not realized. Our consideration shows that this form of *D(d)* relation stems from the Z–shaped relationship between normal-to-front velocity and front curvature $D_n(K)$, which has two turning points. We have got this Z-shaped curve by using a simple model of steady nonideal detonation, including the conversion rate equation with a two-term pressure function. Here the first term with the pressure exponent near 1 is responsible for the surface burning under conditions typical of low velocity detonation, and the second term with the pressure exponent more than 2 controls chemical conversion under normal detonation pressures. Varying coefficients of this function we have reproduced numerically *D(d)* relation with two separate branches observed in unconfined charges of powdered high explosives. We also demonstrate that the Z–shaped $D_n(K)$ relationship could explain some delayed transient effects which have been observed in shock initiation of explosive materials and, to date, have no clear interpretation.

A GENERALIZED DEPENDENCE OF DETONATION VELOCITY ON CHARGE DIAMETER INCLUDING LOW VELOCITY DETONATION

INTRODUCTION

Dependence of detonation velocity on charge diameter *D(d)* is one of the principle characteristics of high and non-ideal explosives which in particular is used to extract data on chemical conversion rates. According to experimental data available for high explosives [1–4], *D(d)* relation comprises two separate branches for low velocity (typically, nearby 1–2 km/s) and normal detonations. In an intermediate velocity range steady detonations were not observed. There is a range of charge diameters in which both low velocity and normal detonations could be observed depending on initiation energy.

Fig. 1 shows a representative example of experimental data on *D(d)* relation obtained in [1] for TNT in unconfined charges of loose-packed density. In these runs in addition to the charge diameter the velocity of entering wave produced by the booster was also varied. There was no detonation initiation observed at charge diameters of 22.2 mm and less irrespective of the entering wave velocity and at the charge diameters of 25.4 mm and more if the entering wave velocity was below the threshold values shown by line 1. The points corresponding to a steady detonation are separated into two branches. Three upper points with the detonation velocities of 3.4, 4.1 and 4.4 km/s correspond to the normal detonation branch. To get them the initiating wave velocity should be above the line 2 (at the charge diameters 25.4–30.2 mm) and above the line 1 (at the charge diameters more than 30.2 mm). Low velocity detonation branch (LVD) consists of points with detonation velocity of 1.7 and 1.9 km/s at diameters of 25.4 and 30.2 mm. To get them, the initiating wave velocity was between the lines 1 and 2.

For other high explosives (RDX, Tetryl and PETN – see [2–4]) the dependence *D(d)* has the same form as above with the aforesaid typical properties: (i) no detonation observed with intermediate velocities; (ii) there is a range of charge diameters in which, depending on intensity of the initiating impulse, one can get a steady detonation propagating with high or low velocity.

Though theoretical principles of LVD are well studied and discussed, up to now the problem of *D(d)* relation consisting of two separate branches has no adequate consideration. The situation can be exemplified by the paper [5] in which the authors, famous specialists in non-ideal detonations, after detailed analysis of experimental data for Tetryl presented in [2] could not offer a satisfactory interpretation and include the low velocity branch into the unique *D(d)* relation calculated numerically.

In this work the conditions necessary for a theoretical model to predict the generalized *D(d)* relation with two separate branches have been considered. A model of the steady detonation developed on the base of classical quasi–1D approximation for weakly diverging flow of two-phase reactive medium has been applied to the analysis of experimental data available. Then, by the best fitting of the calculated and experimental *D(d)* curves we deduced the coefficients of the reaction rate equation which enable one to consider the processes taking place in the LVD waves.

Numerical analysis results in the Z-shaped curve for a velocity–curvature relationship with two turning points. The Z-shaped relationship, being applied to unsteady phenomena, enables us to shed light on some delayed transient effects (including the so-called “delayed detonation”) [2, 6–8] which have been observed in shock and electrical initiation of explosive materials, and, to date, have no clear interpretation. To demonstrate these effects numerical modeling of the spherical diverging detonation has been presented.

MODEL

Let us consider the steady reaction zone of a self-sustained detonation which propagates with a constant velocity D along the axis of unconfined cylindrical charge of an explosive material of diameter d. We interpret LVD as a particular kind of a steady non-ideal detonation, which characteristics (relatively low values of detonation velocity and pressure) relate to features of the chemical conversion rate. Analysis has been conducted in the frame of the detonation shock dynamic approximation (assuming that the velocity normal to the front D_n is a function of the local front

curvature K, and flow in the reaction zone is weakly divergent) [9]. If the curvature–normal velocity relationship K–D_n is known for a high explosive, $D(d)$ relation can be deduced by the following procedure. For the given detonation velocity D, simple geometry consideration for a steady curved wave leads to the following differential equation for the shock front shape $Y(r)$ [10]:

$$Y'' = (1 + Y'^2)[K(1 + Y'^2)^{1/2} - Y'/r] \qquad (1)$$

with a boundary condition at the charge axis:

$$r = 0: \quad Y = Y' = 0 \qquad (2)$$

In equation (1) K is the function $K(D_n)$ with D_n related to D by

$$D_n = D/(1+Y'^2)^{1/2} \qquad (3)$$

Equation (1) is integrated from $r = 0$ up to a point r^*, in which the relevant particle velocity at the wave front becomes equal to the sound speed (C_f):

$$C_f^2 = U_f^2 + D^2/(1+Y'^{-2}) \qquad (4)$$

This point assumes to be the edge of the flow and defines the charge diameter $d = 2r^*$ corresponding to the considered detonation velocity D. Then the same calculations repeat for the other value of D, etc.

It is well-known that the shape of $D(d)$ curve and its characteristics (deficit of detonation velocity, critical detonation diameter, etc.) depend on the shape of the D_n–K relationship. In order to have $D(d)$ relation with two separate branches, D_n–K relationship should have a Z-shape with two turning points; Fig 2 shows an example of this relationship. The intermediate branch of this relationship along which velocity increases with the front curvature covers a range of velocities which cannot be realized in a steady detonation wave because of obvious instability of such behavior in regard to any perturbations at the front. So, we come to the following tasks: (i) to state a form of the reaction rate equation necessary to get the Z-shaped D_n–K relationship, and (ii) to select coefficients of this equation to reproduce $D(d)$ curves observed experimentally. Below we shall demonstrate solution of these tasks by analyzing results of numerical modeling.

Our model developed for the analysis and presented elsewhere [11, 12] relies upon the theory of multiphase reactive medium [13]. Basic assumptions of the model are as follows. The reactive medium is a mixture of the initial explosive component (index 1) and products of their final chemical conversion (index 2). The state of each point of the reactive medium is determined by mass fractions of these species (η_i) with the density and internal energy of the mixture calculated from density (ρ_i) and internal energy (e_i) of these species by the additivity rule. The species are in local mechanical equilibrium, that is, they have identical pressure P and material velocity U but different temperatures.

Let us consider an elementary stream tube in the reaction zone behind the curved wave front with the total curvature K and normal velocity D_n. Along the axis of this stream tube ($x \geq 0$) normal to the wave front, one can deduce the following equation set:

$$\frac{d}{dx}(\rho U) = -\rho U \frac{d}{dx}(\ln S);\ \rho U \frac{dU}{dx} + \frac{dP}{dx} = 0;\ \frac{d(e)}{dx} - \frac{P}{\rho^2}\frac{d(\rho)}{dx} = 0 \qquad (5\text{–}7)$$

$$\rho U \frac{d}{dx}(\eta_1) = -M;\ \frac{de_1}{dx} - \frac{P}{\rho_1^2}\frac{d\rho_1}{dx} = 0 \qquad (8\text{–}9)$$

$$e = \sum \eta_i e_i;\ 1/\rho = \sum \eta_i/\rho_i;\ \sum \eta_i = 1,\ i = 1, 2 \qquad (10\text{–}12)$$

$$P = \Gamma_1 \rho_1 (e_1 - e_{01}) + B_1[(\frac{\rho_1}{\rho_{10}})^l (1 - \frac{\Gamma_1}{l-1}) - \Gamma_1 - 1 + \frac{\rho_1}{\rho_{10}}\frac{\Gamma_1 l}{l-1}] \qquad (13)$$

$$P = \Gamma_2 \rho_2 (e_2 - e_{02}) + B_2 \rho_2^m (1 - \frac{\Gamma_2}{m-1}) \qquad (14)$$

Here (5–9) are the conservation equations of mass, momentum and energy of the mixture and for mass and energy of the initial material; the equations (10–11) express internal energy e and density ρ of the mixture as a function of energy, density and mass fractions of the components η_i in accordance with the additivity rule; (12) is the normalization rule of the mass fractions of the components; (13) and (14) are the equations of state of the components in the Mie-Gruneizen form. Additional designations: S is the area of cross-section of a flow tube, M is intensity of chemical conversion, Γ is Gruneizen coefficient, the index "0" designates the initial conditions, and heat effect of the reaction equals to $(e_{01}-e_{02})$.

The right part of the equation (5) is the term responsible for the flow divergence effect. Assuming that the radius of the front curvature is much greater than the reaction zone length, and following [10], one can write

$$\frac{d}{dx}(\ln S) = (D_n / U - 1)\frac{K}{1 - Kx/2} \qquad (15)$$

Coefficients of the EOS of solid (13) are determined using the literary data on Hugoniot and Gruneizen coefficient. The coefficients of the EOS of detonation products (14) are fitted to get the best approximation of CJ detonation parameters calculated by using the thermodynamic code [14] with the BKWC EOS for the initial densities of explosive material varied in a range covering the detonation pressures expected in normal and low velocity detonations. Fig. 3 shows an example of calibration for coefficients of gaseous EOS.

Boundary conditions at the wave front (at $x = 0$) are assumed to be the common conservation equations at the shock discontinuity:

$$\rho_o D_n = \rho_f U_f;\ P_f = \rho_o D_n (D_n - U_f);\ e_f = e_o + (D_n - U_f)^2 / 2 \qquad (16)$$

From a physical viewpoint they suggest that the relaxation processes taking place during shock loading of a porous explosive material and resulting in mechanical equilibrium are much faster (their duration may be estimated by use of a characteristic time of pore collapse which equals $4\mu/P_f$ [15], where μ is the effective viscosity of solid explosive) than the chemical conversion time. Pore collapse is accompanied by a dissipative heating of pore surface layers and formation of hot spots. For high explosives of loose-packed density at a pressure exceeding a threshold value P_{ign} (this value typically equals several hundreds MPa) the temperature in hot spots reaches a value sufficient to begin fast chemical reactions. Both the chemical reactions in hot spots and filling of pores with reaction products which contribute into pressure relaxation at a meso–scale level are main components of the shock loading process of porous HE and should be attributed to the wave front. According to the theoretical analysis [15], only several percents of HE are consumed in hot spots (η_{2f} in our designations). The delay of reaction initiation in hot spots quickly drops with increase of the wave amplitude, and already at amplitudes P_f exceeding the threshold value P_{ign} by several tens of percents, the sum of the initiation delay and duration of reactions in hot spots occupies less than a half of the characteristic time of pore collapse. A detailed analysis of η_{2f} and its dependence on shock pressure is beyond this study; here we conducted calculations with η_{2f} being constant and equal to 2 %. We have preliminary varied the value of η_{2f} to be sure that it does not affect appreciably the results of modeling. This physically significant parameter in addition eliminates the singularity of the equation set at the initial point.

So, chemical conversion in the reaction zone begins without a delay just behind the wave front. At low pressures specific of LVD, the chemical conversion proceeds in the surface (explosion) burning mode [16]. For this case, intensity of chemical conversion M can be expressed as the product of specific surface area and rate of burning (regression); it results in M being a function of the reactant content and pressure. Relying upon extrapolation of experimental data on the layer-by-layer burning of HE in sticks, this pressure dependence is assumed to be close to linear. For a normal detonation, the contribution of volume reactions is more significant. Nevertheless, even in this case the formal law of reaction rate can be presented as a function of the reactant content and pressure. For these reasons we have used in our model the following two-term equation which formally coincides with the Forest Fire equation [17]:

$$M_1 = \rho_{10}(\eta_1/\eta_{10})^{2/3} G_1[(P/P_{ref})^n + g(P/P_{ref})^k] \qquad (17)$$

Here the pressure P_{ref} is set equal to 1 GPa and introduced for convenience in order to express the burning coefficient G_1 in sec^{-1} irrespective of the pressure exponents. Three other coefficients (pressure exponents n and k, and non-dimensional coefficient g), being varied, enable one to select a desirable form of D_n–K relationship. Equation (17) holds if the wave front pressure exceeds the threshold P_{ign} else M_1 is set to 0.

The equation set of the model comprises 10 equations for 12 variables. By transformation of the equations one may obtain the master equation of the standard form:

$$\frac{dU}{dx} = \frac{M_1 \dfrac{[\kappa_2(1-\rho_2/\rho_1)+\Gamma_2(e_1-e_2)]}{(\kappa_2\rho_2+P\Gamma_2)} - \dfrac{(D_n-U)K}{1-Kx/2}}{(1-U^2/C^2)} \qquad (18)$$

Here the functions $\kappa_i = \partial P/\partial\rho_i\big|_{e_i}$ are deduced by differentiation of EOS of the species, and the sound speed is:

$$C = \left\{\rho^2\left[\frac{\eta_1}{\rho_1(\rho_1\kappa_1+P\Gamma_1)} + \frac{\eta_2}{\rho_2(\kappa_2\rho_2+P\Gamma_2)}\right]\right\}^{-1/2} \qquad (19)$$

Two terms in numerator of the right part of the equation (18) represent heat release rate by chemical reaction and energy losses rate caused by lateral expansion, accordingly. The equation set is integrated from the shock front up to a singular sonic point at which the numerator and the denominator of the right part of the equation (18) simultaneously equal zero. The unique solution which begins at x=0 and passes through this singular point, defines an eigenvalue of the problem. It may be velocity D_n at a given curvature, or reverse. The solution is obtained by use of a numerical "shooting" technique. Fig. 4 shows an example of the procedure.

RESULTS OF ANALYSIS

Numerical modeling carried out with use of one-term equation for reaction rates (at g = 0 in the equation (17)) and with variation of the pressure exponent results in D_n–K relationship which has one turning point at $n \geq 1.7$ or the monotonously descending relationship with no turning points at the smaller values n. The D_n–K relationship with two turning points may be obtained with use of the two-term equation (17) if n is nearby 1 and k above 2.5. By taking these values of the pressure exponents we have reproduced experimental data on $D(d)$ relation including low velocity branch for three powdered HEs [3–4]. Figs. 5–7 show the obtained results. The input data comprising coefficients of EOS and reaction rate equation are listed in Tables 1 and 2, accordingly. The experimental data available for Tetryl demonstrate a strong effect of the particle size. We have numerically reproduced this effect by proportional change of the coefficient G_1.

With regards to the mechanism of explosive burning, coefficient G_1 may be estimated as the product of the specific burning surface and the rate of layer-by-layer burning of HE at the reference pressure 1 GPa. We have taken values of the burning rate measured for sticks under lower pressures and extrapolated them with the pressure exponent equal 1. The specific burning surface is assumed to be equal to the specific surface of initial particles. The results of this simple estimation are shown in Table 2. One can see that the chemical reaction rates extracted by use of numerical modeling significantly exceed the values estimated by extrapolation.

Figs. 8–9 illustrate spatial profiles of variables along the charge axis as well as the front shape and pressures at the front calculated for LVD propagating with the wave velocity 1.85 km/s in the unconfined RDX charge of 16 mm in diameter. As it is typical of LVD, due to the relatively low reaction rate only 40 % of HE is consumed in the reaction zone before the sonic locus. Comparing the reaction zone length with the charge diameter or the radius of curvature and considering the flow tube

expansion, we have to conclude that the assumption of the model about the weakly divergent flow does not strictly hold. And although the results of our study correctly reflect real physical aspects of detonation and give proper qualitative understanding of the process, quantitative data for the coefficients of the reaction rate equation are to be elaborated. For this purpose more sophisticated models may be applied (for example, the approach presented in [18] or 2D gas-dynamic modeling).

UNSTEADY EFFECTS

Chemical reactions occurring in the LVD waves manifest themselves also in the course of transient processes. We may qualitatively illustrate possible effects and consider the evolution of a diverging spherical detonation by using D_n–K relationship with two turning points.

According to Brun [19], the acceleration of a self-sustained spherical divergent detonation is given by the relation:

$$\frac{dD}{dt} = 2C_{tr}^2[K(D) - \zeta] \qquad (20)$$

Here D is the local detonation velocity, C_{tr} is the characteristic speed of transverse front waves, $K(D)$ is the known function of the local detonation velocity, and ζ is the curvature of the front. With R being the local radius of the spherical detonation,

$$\zeta = 2/R \qquad (21)$$

Assuming for simplicity that

$$C_{tr}^2 = 0.6D^2 \qquad (22)$$

we come to the following equation set for the trajectory of the spherical detonation:

$$\frac{dD}{dR} = 2C_{tr}^2[K(D) - 2/R]/D \qquad (23)$$

$$\frac{dt}{dR} = 1/D \qquad (24)$$

with initial conditions at $R = R_0$: $D = D_0$, $t = 0$.

Fig. 10 shows the calculation results for RDX of loose-packed density at various initial radius of the wave R_0. Initial velocity D_0 was constant and equal 4 km/s, that corresponds to the radius of curvature 7.8 mm defined from the available $K(D)$ relationship. At R_0 = 6 mm the wave develops almost without drop of velocity, and after several microseconds the level of normal detonation velocity is reached. At R_0 = 2 mm, the detonation quickly failed because the initial curvature of the front is too large. At R_0 = 2.2 mm the wave velocity also undergoes a sharp drop. However, due to contribution of slow reactions initiated behind the front of low-velocity wave, parameters of the wave holds above a critical level. After a 12 μs delay when radius of the wave front increases up to ~20 mm the wave abruptly accelerates up to the velocity of normal detonation. These results qualitatively reproduce the experimental effects observed by authors of [2, 6]. They investigated the powdered RDX initiated by cap or electrical discharge and observed significant delay to detonation and long run distance to detonation. During delay the wave propagates with average velocity nearby 2–3 km/s and then abruptly transits to normal detonation velocity. Up to now, these effects have no clear explanation.

The similar effects observed in PBX are known as “delayed detonation” [7, 8]. Fig. 11 shows experimental data which demonstrate extremely long delay of detonation and run distance to detonation taking place in a narrow range of the amplitudes of entering wave. By taking into consideration the chemical reactions occurring at low velocity detonations, we can offer a new idea to highlight this phenomenon. And again we consider the evolution of a spherical diverging detonation by using the D_n–K relationship with two turning points. Earlier in [11] we have selected coefficients of EOS and coefficients of the reaction rate equation (17) by using for calibration the experimental data

on LVD obtained in strongly confined charges 16 mm i.d. of X1 (HMX/binder 96/4, density 1.823 g/cm^3) and its normal detonation performance (detonation velocity 8.77 km/s and critical detonation diameter 2 mm) [20]. The coefficients of the reaction rate equation are G_1=0.0012μs^{-1}, n=1.0, f=0.3 and k=3.5. Fig 12 shows the resulting Z-shaped velocity–curvature relation, and Fig. 13 displays the evolution of detonation wave depending on the pressure amplitude P_0 of initial wave (P_0 is a known function of D_0) with the initial radius R_0 = 32 mm keeping constant. One may notice a qualitative agreement with the experimental data, specifically, the change of the prompt transition mode to a mode with 60-μs delay in the narrow 6.44–6.7 GPa interval of P_0, a low-velocity stage propagating with nearby 2.5 m/s and a jump-like transition from the low velocity to the normal detonation mode.

CONCLUSIONS

According to experimental data available for both confined and unconfined high explosives, dependence of detonation velocity on charge diameter *D(d)* comprises two separate branches for low velocity and normal detonations. Low velocity detonation is a wave process governed by chemical reactions which occur under dynamic loading with low amplitudes of the order of 1 GPa. A correct consideration of these reactions is necessary for a progress of the detonation theory as well as for understanding transient effects of initiation and failure of a detonation. Our numerical analysis have revealed simple conditions at which the steady model of a non-ideal detonation can reproduce *D(d)* relation comprising two separate branches for low velocity and normal detonations observed experimentally. This form of *D(d)* relation stems from Z-shaped normal velocity – curvature relationship which, in turn, can be obtained if the pressure dependence of the reaction rate comprises two terms. Namely, the first term is responsible for the surface burning under pressures typical of LVD with the pressure exponent nearby 1, and the second term controls chemical conversion under normal detonation pressures and has the pressure exponent 2.5–3. By fitting coefficients of the reaction rate equation, we have numerically reproduced *D(d)* relation with two branches for several high explosives in unconfined charges of loose-packed density, including the particle size effect.

We also applied the Z-shaped velocity–curvature relationship for considering unsteady delayed transient effects (including the so-called “delayed detonation”) which have been observed at shock initiation of explosive materials and have no clear interpretation. To demonstrate these effects a numerical modeling of the spherical divergent detonation is presented.

Though modeling results are in good agreement with the experimental data, we estimate them as qualitative or illustrative rather than quantitative ones. The reason is that due to the low reaction rate peculiar to LVD, the reaction zone length can not be considered as negligibly small in comparison to the radius of curvature. As a consequence the assumption of weakly divergent flow which enables us to apply the simple classic procedure for the analysis does not strongly hold. Nevertheless, we believe that the results of our study give proper understanding of the phenomenon and will be useful as a basis for developing more sophisticated and adequate models.

LIST OF REFERENCES

1) Jones E., and Cumming G. (1955) *Sensitiveness to Detonation* // 2nd ONR Symp. on Detonation, P. 483.

2) Cook M.A., Keyes R.T., Partridge W.S., and Ursenbach W.O. (1957) *Velocity-Diameter Curves, Velocity Transients and Reaction Rates in PETN, RDX, EDNA and Tetryl* // Journal of the American Chemical Society, V.79, P. 32.

3) Parfenov A.K. and Apin A.Ya. (1965) *About a detonation with low velocity in powdered HE* // Fizika goreniya i vzryva, № 1б, P. 109.

4) Parfenov A.K., and Voskoboynikov I.M. (1969) *Low velocity detonation in powdered HE* // Physics of burning and explosion, V. 5, P. 347.

5) Leiper G. A. and Cooper J. (1995) *Low and High Order Detonation in Tetryl* // Propellants, Explosives, Pyrotechnics, V. 21, Issue 6, P. 325.

6) Muller G.M., Moore D.B. and Bernstein D (1960) *Electrical initiation of RDX* // Third Symp. on Detonation, 26-28 Sept. 1960, ONR, ACR-52, P. 88.

7) Salvetat B. and Guery G.F. (1993) *Visualisation and Modelling of Delayed Detonation in the Card Gap Test* // 10th Int. Det. Symp., July 12-16, P. 709, ONR 33395-12.

8) Bernecker R.R., Clairmont-Jr A.R., and Hadson 111 L.C. (1993) *Prompt and Delayed Detonation from Two-Dimensional Shock Loadings* // 10th Int. Det. Symp., July 12-16, P. 476, ONR 33395-12.

9) Bdzil J. and Stewart D.S. (1989) *Modeling Two-Dimensional Detonations with Detonation Shock Dynamics* // Phys. Fluids, A 1, P. 1261.

10) Swift D.C, and Lambourn B.D. (1993) *A Review of Developments in the W-B-L Detonation Model //* 10th Int. Det. Symp., July 12-16, P. 386, ONR 33395-12.

11) Ermolaev B.S., Khasainov B.A., Presles H.-N., and Vidal P. (2005) *A Simple Approach for Modelling Reaction Rates in Shocked Multi-Component Solid Explosives //* Proceed. European Combustion Meeting (ECM2005), Lourain-la-Neuve, Belgium, April 3-6, 2005.

12) Ermolaev B.S., Khasainov B.A., Presles H.-N., Vidal P., and Sulimov A.A. (2005) *Low velocity detonation in ammonium nitrate and its mixtures. //* X111 Russian Symp. on combustion and explosion, Chernogolovka, Moscow region, 7–11 Febr. 2005, report No 155.

13) Nigmatulin, R. I. (1987) *Dynamics of Multi-phase Media.* // Nauka Press, Moscow (in Russian).

14) Victorov S.B. (2002) *The Effect of Al2O3 Phase Transitions on Detonation Properties of Aluminized Explosives* // 12th Int. Det. Symp., August 11 - 16th, San Diego, Ca.

15) Khasainov B.A., Attetkov A.V., and Borisov A.A. (1996) *Shock-wave Initiation of Porous Energetic Materials and Visco-Plastic Model of Hot Spots* // Chem. Phys. Reports, V. 15 (7), P. 987.

16) Apin A.Ya. (1950) // Doklady Akademii Nauk SSSR, V.50, P.285 (in Russian).

17) Mader Ch. L. (1979) *Numerical modeling of detonations* // Univ. of California Press. Berkeley.

18) Stewart D.S., and Yao J. *The normal Detonation Shock Velocity – Curvature Relationship for Materials with Nonideal Equation of State and Multiple Turning Points //* Combustion and Flame, 1998, v.113, No 1-2, p.224-235.

19) Brun, L., Kneib, J.-M., and Lascaux, P. (1993) *Computing the Transient Self-Sustained Detonation after a New Model* //10th Int. Det. Symp., Boston, Ma., July 12-16, ONR 33395-12, P. 43.

20) Leuret F., Chaisse F., Presles H.N., and Veyssiere B. (1998) *Experimental Studies of the Low Velocity Detonation Regime during the Deflagration to Detonation Transition in a High Density Explosive //* 11th Int. Det. Symp., August 31–Sept. 4, Snowmass, Co, ONR 333000-5, P. 693.

TABLES AND FIGURES

Table 1. Input data for coefficients of EOS

HE	Coefficients of Eq. (13), KEOS					Coefficients of Eq. (14), GEOS			
	ρ_{10}, kg/m^3	e_{10}, MJ/kg	Γ_1	l	B_1, GPa	e_{20}, MJ/kg	Γ_2	m	B_2
RDX	1800	+ 0.028	2.6	7.4	2.0	-5.0	0.35	3.23	0.59
Tetryl	1730	+ 0.068	1.65	7.45	1.09	-4.47	0.5	3.121	1.0841
TNT	1650	- 0.276	0.74	6.9	1.366	-4.4	0.5	3.513	0.0473

Table 2. The best fitting values of coefficients of the reaction rate equation (17) to reproduce experiments on effect of charge diameter on low velocity and normal detonations [3, 4]

HE	ρ_0, kg/m^3	d_0, mm	G_1, μs^{-1}	$n/g/k$	U_P, m/s (1 GPa)	$U_P A_0$, μs^{-1}
TNT	950	0.4 – 0.63	0.04	1.0/0.37/3.0	0.43	0.005
RDX	1000	1.0 – 1.6	0.061	1.0/0.38/2.5	1.14	0.0053
Tetryl	900	0.4 – 0.63 0.63 – 1.0 1.0 – 1.6	0.11 0.085 0.065	0.8/0.26/2.7	0.57	0.0066 0.0042 0.0026

*) Specific surface of grains: $A_0 = 6/d_0$

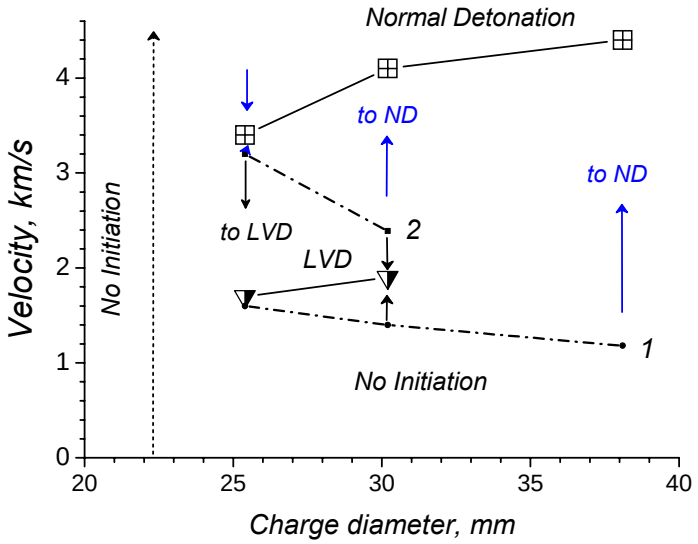

Fig. 1. Experimental data on low-velocity (LVD) and normal detonations (ND) in powdered TNT of 1000 kg/m^3 in density [1]. Initiation by means of boosters producing different velocity of the input wave.

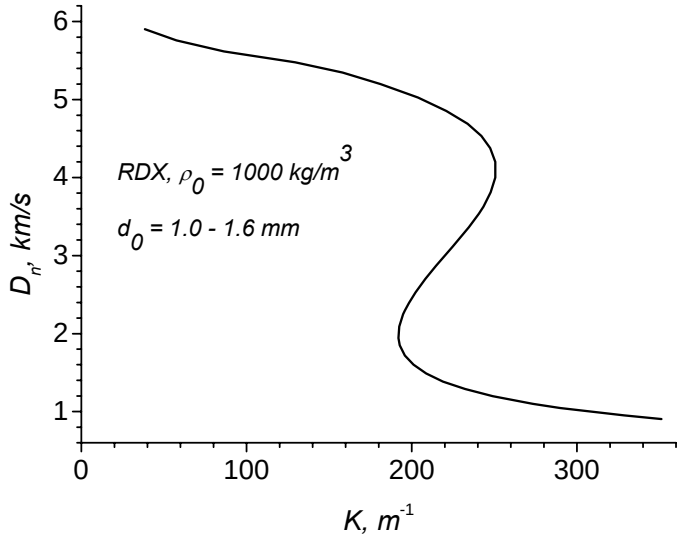

Fig.2. Example of Z-shaped normal velocity–curvature relationship with two turning points

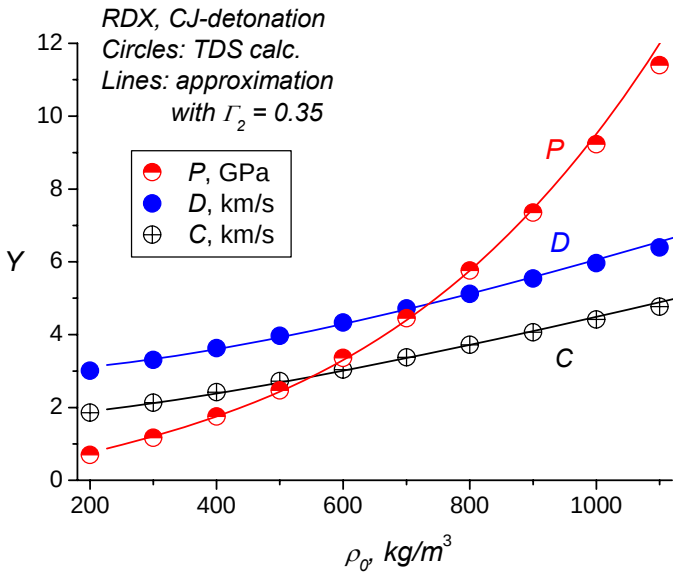

Fig. 3. Example of calibration of the EOS coefficients. Circles are thermodynamic calculation by TDS, lines are calculations by equation (13).

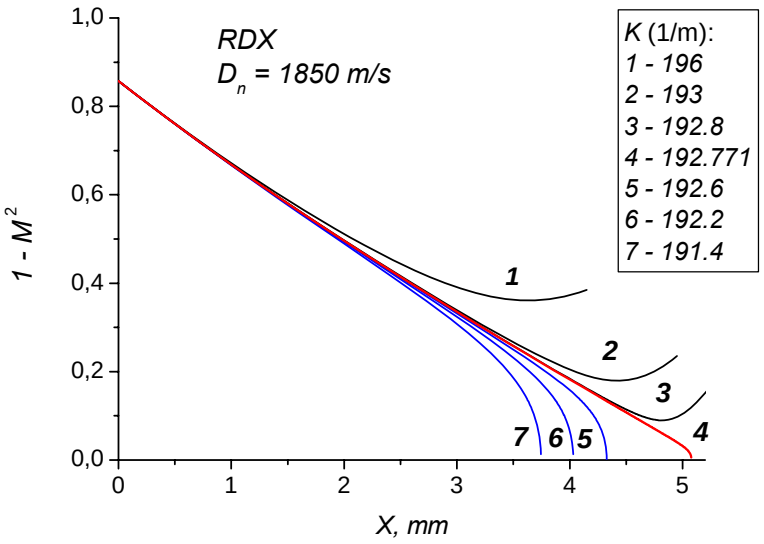

Fig. 4. An example of "shooting" procedure

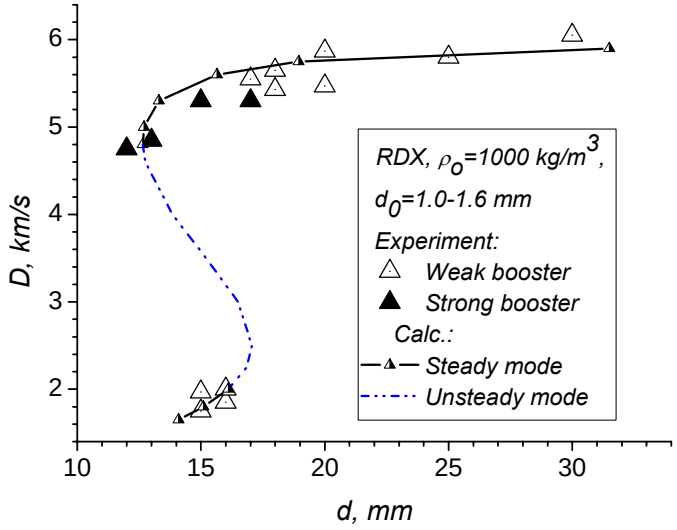

Fig. 5. Experimental and calculated detonation velocity – charge diameter relation for unconfined powder RDX

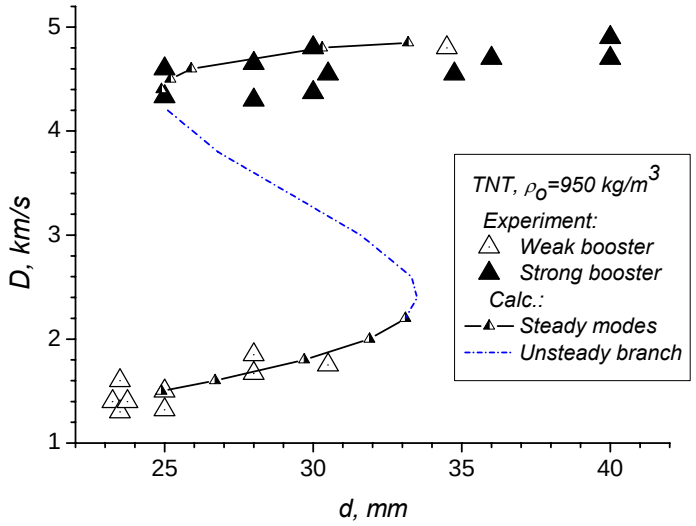

Fig. 6. Experimental and calculated detonation velocity – charge diameter relation for unconfined powder TNT

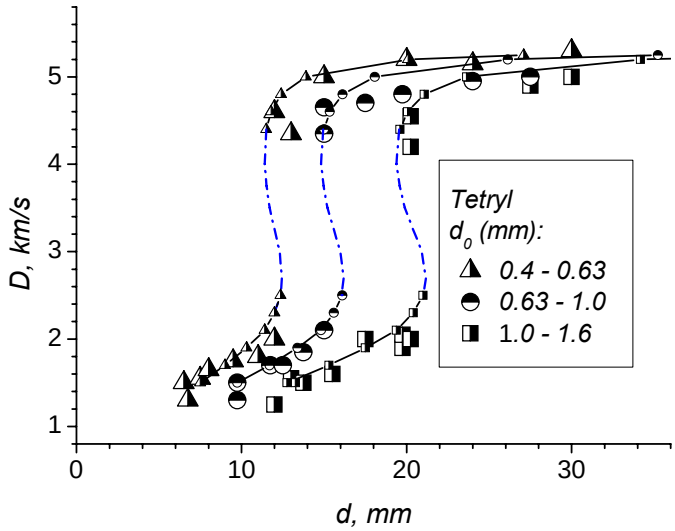

Fig. 7. Experimental and calculated detonation velocity – charge diameter relation for unconfined Tetryl with different particle size

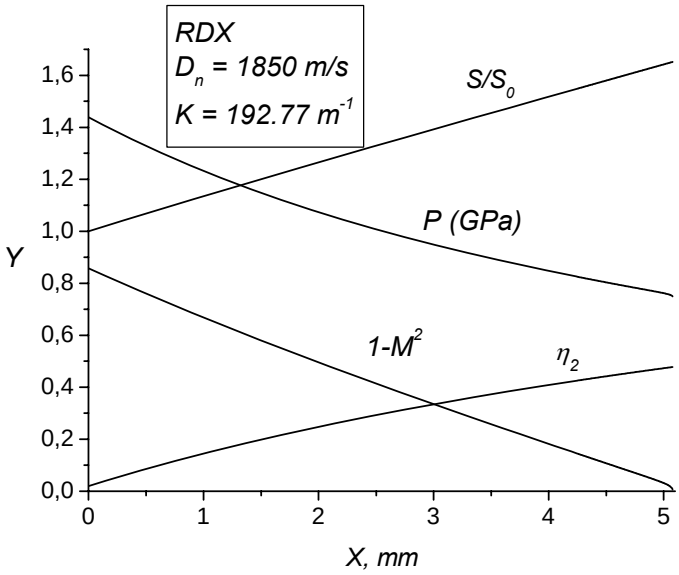

Fig. 8. An example of spatial profiles of variables in the reaction zone of LVD along the charge axis

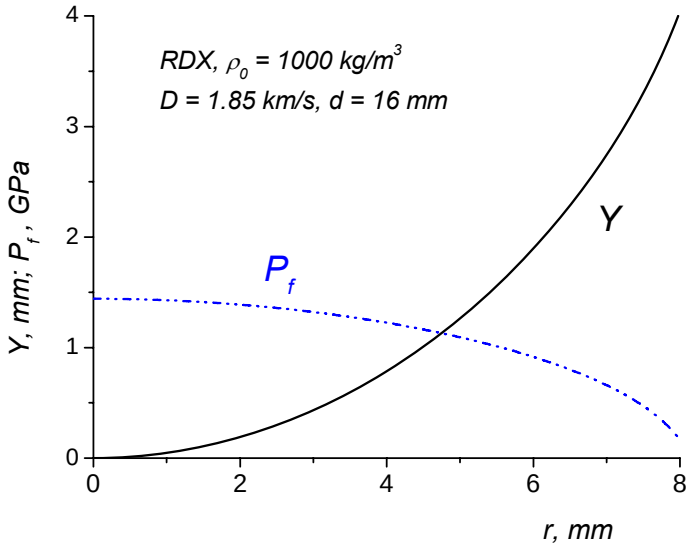

Fig. 9. Front shape and pressure along the shock front for LVD

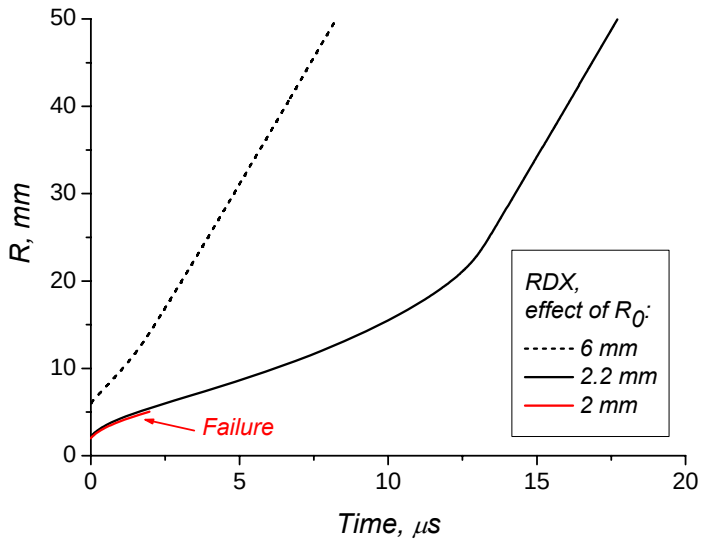

Fig.10. Evolution of spherical detonation front in powdered RDX depending on initial radius.

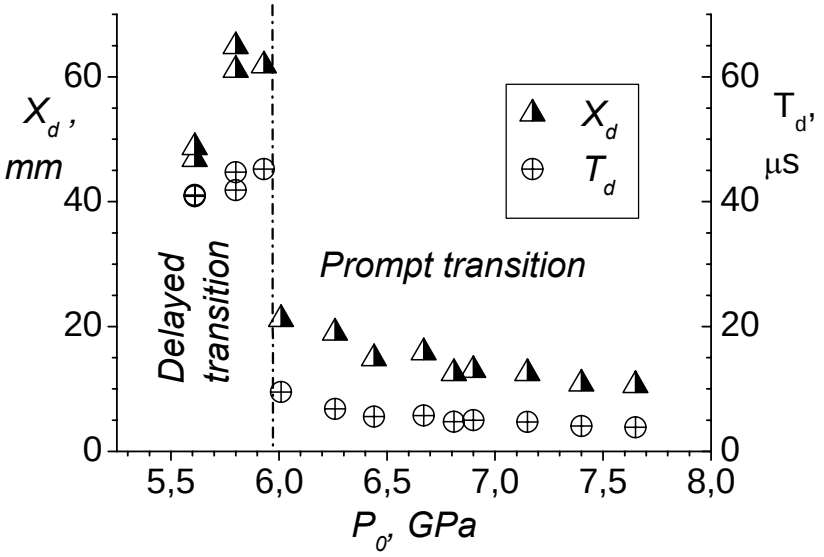

Fig. 11. Effect of the entering shock pressure on the distance to detonation (X_d) and time to detonation (T_d) in unconfined PBX [8]

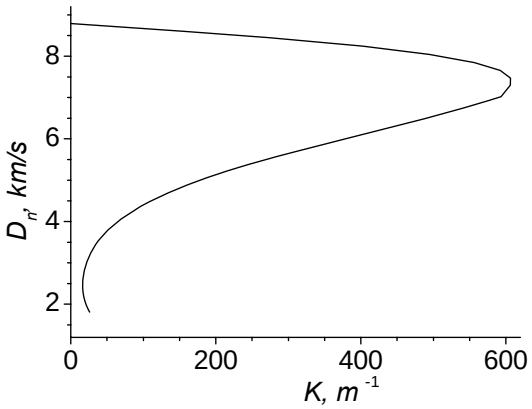

Fig.12. The Z-shaped velocity – curvature relationship fitted for a model PBX

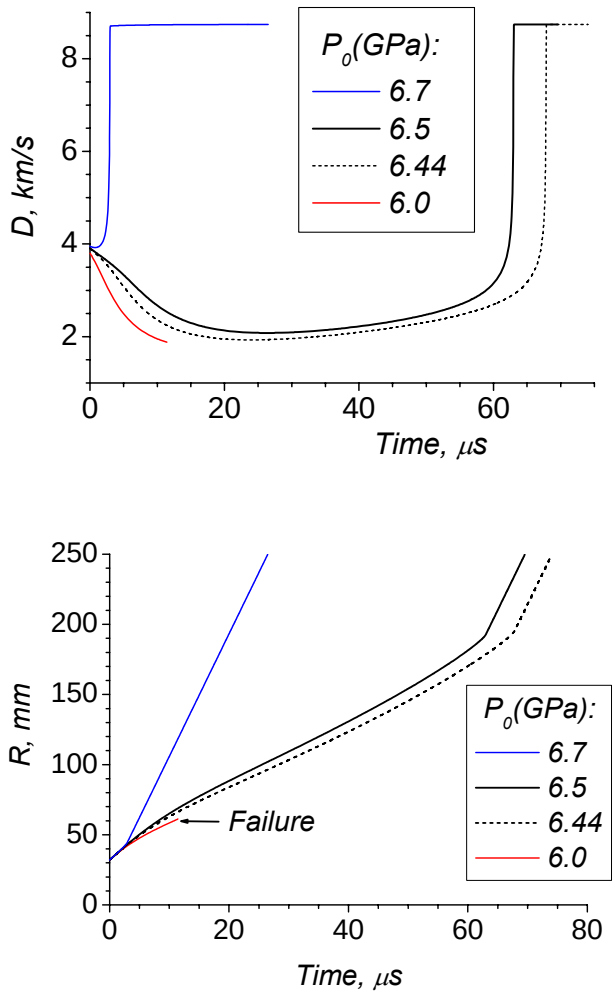

Fig 13. An illustrative example of fast and delayed evolution of a diverging spherical detonation in an unconfined charge of a model PBX with initial radius 32 mm depending on pressure amplitude P_0 of initial detonation wave.